

Isomeric Cross-Section Ratios for Reactions Producing the Isomeric Pair $\text{Hg}^{197,197m\ddagger}$ R. VANDENBOSCH AND J. R. HUIZENGA
Argonne National Laboratory, Argonne, Illinois

(Received July 11, 1960)

Excitation functions and isomeric cross-section ratios were determined for the $\text{Au}^{197}(p,n)$ and $\text{Au}^{197}(d,2n)$ reactions. Isomeric cross-section ratios were also determined for the $\text{Hg}^{196}(n,\gamma)$, $\text{Hg}^{196}(d,p)$, $\text{Hg}^{198}(n,2n)$, $\text{Hg}^{198}(\alpha,\alpha n)$, and $\text{Pt}(\alpha,\alpha n)$ reactions. Those reactions for which compound nucleus formation predominates are treated by a statistical model. In this treatment the compound state is characterized by angular momentum and excitation energy. The analysis yields a value of 4 ± 1 for the parameter σ which characterizes the dependence of the nuclear level density on angular momentum. Relatively small amounts of angular momentum are transferred in reactions which proceed predominantly by a direct interaction mechanism. Such reactions, therefore, give a larger yield of the isomer with spin closer to that of the target nucleus.

1. INTRODUCTION

THE purpose of the present work was, (1) to make detailed and extensive measurements of the isomeric cross-section ratios for the same isomeric pair produced in a large variety of reactions and (2) to explore quantitatively the significance of some of these results in terms of the angular momentum transfer in the initial interaction and the modification of this angular momentum by the sampling of the spin dependence of the nuclear level density by particle and gamma-ray emission. Such analyses of the experimental cross-section ratios yield valuable information on the spin dependence of the nuclear level density, especially if one considers reactions where particles are emitted which can carry off enough angular momentum to reach many spin states of the residual nucleus.

The distribution in spins is predicted theoretically^{1,2} to be of the form

$$\rho(J) = \rho(0) (2J+1) \exp[-(J+\frac{1}{2})^2/2\sigma^2], \quad (1)$$

where $\rho(J)$ is the density of levels with spin J , $\rho(0)$ is the density of levels with zero spin, and σ is the parameter characterizing the distribution function. Little is known experimentally about σ , although some information is available from counting of states^{3,4} and from analysis of angular distributions.⁵

2. EXPERIMENTAL PROCEDURE

A summary of the different types of irradiations performed appears in Table I.

For the $\text{Au}^{197}(p,n)$, $\text{Au}^{197}(d,2n)$, and $\text{Pt}(\alpha,\alpha n)$ excitation function measurements, thin metallic foils (0.1 to 0.6 mil) were placed between aluminum degrading foils of known thickness. The foil stacks were exposed to the deflected beam of the Argonne 60-in. Cyclotron. The

target holder served as a Faraday cup and the current collected was integrated with an uncertainty of less than 2%. Range measurements were made with an absorber wedge to determine the energy of the beam particles. Mean ranges were converted to particle energies using the proton range-energy measurements of Bichsel.^{6,7} Range-energy curves for deuterons and helium ions were constructed from the proton ranges using the assumption that the energy loss $-dE/dx$ has the same velocity dependence $F(v)$ for different particles, so that $R = M/Z^2 F(v)$.

The targets used for the determination of isomeric cross-section ratios in the $\text{Hg}^{196}(d,p)$ and $\text{Hg}^{198}(\alpha,\alpha n)$ reactions were prepared by slurring HgS powder onto an aluminum plate with a solution of Zapon in acetone. After the acetone evaporated, the Zapon held the HgS powder firmly enough to enable mounting in a target holder and subsequent removal from the target holder after irradiation. The target material used in the study of the $\text{Hg}^{196}(d,p)$ reaction was enriched in Hg^{196} .

The irradiation for the measurement of the isomeric cross-section ratio for the $\text{Hg}^{196}(n,\gamma)$ reaction was performed in the thermal flux of the Argonne Reactor CP-5. Mercury of naturally occurring isotopic abundance was irradiated in the form of mercuric sulfide. The 14.1-Mev neutrons in the $\text{Hg}^{198}(n,2n)$ reaction were obtained from

TABLE I. Summary of conditions for measurements of relative production of Hg^{197} and Hg^{197m} .

Target	Material	Reaction	Number of energies	Energy range
Au^{197}	Foil	(p,n)	5	7.3–10.4 Mev
Au^{197}	Foil	$(d,2n)$	20	7.2–21.4 Mev
Pt	Foil	$(\alpha,\alpha n)$	6	18.4–27.3 Mev
Hg	HgS	(n,γ)	1	thermal
Hg	HgS	$(n,2n)$	1	14.1 Mev
Hg^{196}	HgS	(d,p)	1	11 Mev
Hg	HgS	$(\alpha,\alpha n)$	1	41 Mev

[†] Based on work performed under the auspices of the U. S. Atomic Energy Commission.

¹ H. A. Bethe, *Revs. Modern Phys.* **9**, 84 (1937).

² C. Bloch, *Phys. Rev.* **93**, 1094 (1954).

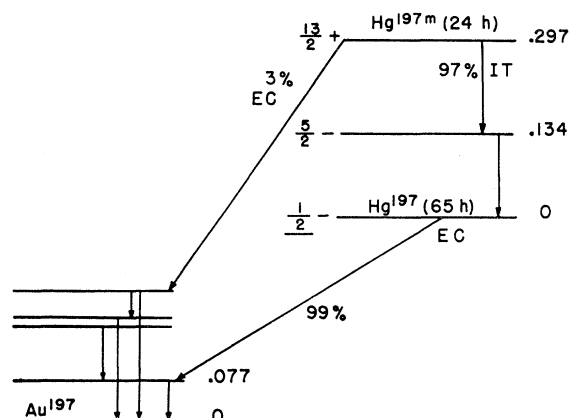
³ C. T. Hibdon, *Phys. Rev.* **114**, 179 (1959).

⁴ T. Ericson, *Nuclear Phys.* **11**, 481 (1959).

⁵ T. Ericson and V. M. Strutinski, *Nuclear Phys.* **8**, 284 (1958), and A. C. Douglas and N. Macdonald, *Nuclear Phys.* **13**, 382 (1952).

⁶ H. Bichsel, *Phys. Rev.* **112**, 1089 (1958).

⁷ H. Bichsel, R. F. Mozley, and W. A. Aron, *Phys. Rev.* **105**, 1788 (1957).

FIG. 1. Principal features of the Hg^{197} , Hg^{197m} decay scheme.

the $\text{T}(d,n)\text{He}^4$ reaction, and mercuric sulfide was the target material.

The foils irradiated for studying the $\text{Au}^{197}(p,n)$ and $\text{Pt}(\alpha,xn)$ reactions were counted without any chemical purification after the irradiation. Because of the large amount of Au^{198} produced by the $\text{Au}^{197}(d,p)\text{Au}^{198}$ reaction, the foils from deuteron irradiations were dissolved and the gold was extracted into ethyl acetate. The mercury was electrodeposited onto silver foils for counting. For the $\text{Hg}^{196}(d,p)$ and $\text{Hg}^{198}(\alpha,\alpha n)$ measurements radiochemical purifications involving anion exchange, solvent extraction and sulfide precipitations were performed to remove gold, thallium, and lead contaminants.

The radiations of the Hg^{197} isomers were detected with a 3×3 sodium iodide (Tl activated) crystal connected with a multichannel pulse-height analyzer. The decay scheme⁸ of the Hg^{197} isomers is very complicated and considerable care must be exercised in interpreting the gamma spectrum. The decay scheme is illustrated in outline in Fig. 1. Two lines are prominent in the spectrum, one at approximately 75 keV and one at 134 keV. The line at 134 keV is attributed to a transition of 24-hr Hg^{197m} decaying to Hg^{197} . The line at approximately 75 keV arises from several processes: (1) K x rays arising from vacancies from the 3% electron capture branch of 24 hr Hg^{197m} , (2) K x rays from internal conversion of the 134- and 164-keV transitions in the decay of Hg^{197m} ,

TABLE II. Isomeric cross sections for the $\text{Au}^{197}(p,n)\text{Hg}^{197,197m}$ reaction.

Proton energy (MeV)	$\sigma_{I=13/2}$ (mb)	$\sigma_{I=1/2}$ (mb)	$\sigma_{I=13/2}/\sigma_{I=1/2}$
7.3	0.4	1.8	0.22 ± 0.02
8.5	3.3	14.2	0.23 ± 0.02
9.4	10.7	41.1	0.26 ± 0.02
9.9	19.9	64.3	0.31 ± 0.03
10.4	26.8	74.9	0.36 ± 0.03

⁸ D. Strominger, J. M. Hollander, and G. T. Seaborg, Revs. Modern Phys. **30**, 585 (1958).

(3) K x rays from the electron capture decay of 65-hr Hg^{197} , (4) K x rays from internal conversion of the various transitions in the daughter Au^{197} , and (5) 77-keV gamma rays from the decay of the first excited state of daughter Au^{197} . At poor geometry (sample close to crystal) one obtains K x-ray- K x-ray and K x-ray-77-keV sum peaks which cannot be resolved from the 134-keV gamma ray. In order to minimize the magnitude of the sum peaks in counting the 134-keV gamma, the samples were counted in a 3.7% geometry. Even so, a small correction was made for the sum peak contribution.

The absolute number of disintegrations of Hg^{197m} may be obtained from the 134-keV photopeak intensity and the measured conversion coefficient⁸ of the transition. It is also possible to calculate the Hg^{197m} contribution to the K x-ray peak from the known K/L ratios and the K conversion coefficients of the two transitions.⁸ When

TABLE III. Isomeric cross sections for the $\text{Au}^{197}(d,2n)\text{Hg}^{197,197m}$ reactions.

Deuteron energy (MeV)	$\sigma_{I=13/2}$ (mb)	$\sigma_{I=1/2}$ (mb)	$\sigma_{I=13/2}/\sigma_{I=1/2}$
7.2	0.3	0.9	0.33 ± 0.03
8.4	3.0	8.6	0.35 ± 0.03
9.5	17.6	44.3	0.40 ± 0.04
10.8	66	129	0.51 ± 0.05
11.1	102	207	0.49 ± 0.05
12.0	125	202	0.62 ± 0.06
12.3	205	344	0.60 ± 0.06
13.9	278	339	0.82 ± 0.08
14.3	250	242	1.03 ± 0.10
14.7	296	303	0.98 ± 0.10
15.6	286	262	1.09 ± 0.10
16.5	251	203	1.24 ± 0.15
16.5	241	196	1.23 ± 0.15
17.9	200	160	1.25 ± 0.15
18.4	156	104	1.50 ± 0.15
19.4	134	119	1.13 ± 0.15
19.7	120	89	1.35 ± 0.15
21.0	1.15 ± 0.10
21.1	92	68	1.35 ± 0.15
21.4	94	90	1.04 ± 0.15

this contribution is subtracted, the remainder of the 75-keV peak is due to 65-hr Hg^{197} . Since the K to L electron capture ratio is not known for Hg^{197} and some of the conversion coefficients for transitions in the daughter Au^{197} are not very well known, it is not possible to obtain the absolute disintegration rate of Hg^{197} directly. Two experiments were performed in which the 75-keV peak of Hg^{197} was observed to grow in from the decay of Hg^{197m} . By appropriate rearrangement of the growth and decay equation one obtains an expression which, when plotted as a function of time, gives a straight line whose intercept gives the ratio of the detection efficiency for the two periods. Thus by using the known efficiency for Hg^{197m} it is possible to obtain the absolute efficiency for detecting Hg^{197} . Two values for the constant relating the two efficiencies were obtained, and the average of these measurements was used in analyzing all of the data obtained in this work. As an

incidental result, if one combines the measured relative efficiency with what is known about the decay scheme, it is possible to estimate the $K/L+M$ electron capture ratio. This ratio was found to be approximately 0.6 and is rather sensitive to uncertainties in conversion coefficients.

3. EXPERIMENTAL RESULTS

The isomeric cross-section ratio produced by thermal neutron activation of Hg^{196} was found to be $\sigma_m/\sigma_g = 0.044 \pm 0.008$. This result is in serious disagreement with a recent measurement by Sehgal *et al.*⁹ The reason for this discrepancy is not obvious, but possibly may be attributed to the fact that the gamma-ray resolution in the present experiment was much better enabling a more accurate determination of the intensity of the rather small 134-keV photopeak.

The $\text{Au}^{197}(p,n)$ and $\text{Au}^{197}(d,2n)$ cross sections are tabulated in Tables II and III. The uncertainty in the projectile energy is ± 0.5 MeV and the uncertainty in the

TABLE IV. Isomeric cross-section ratios for $\text{Pt}(\alpha, xn)\text{Hg}^{197,197m}$ reactions.

Helium ion energy	$\sigma_{I=13/2}/\sigma_{I=1/2}$
18.4	0.35 ± 0.04
20.6	0.67 ± 0.07
22.7	1.00 ± 0.10
24.7	1.47 ± 0.16
25.4	1.59 ± 0.25
27.3	2.5 ± 0.4^a

^a Probably includes contribution of Hg^{195} from $\text{Pt}^{194}(\alpha, 3n)$ reaction which becomes energetically possible at this energy.

absolute value of the cross sections is estimated to be less than 20%. The isomeric cross-section ratios are known somewhat more accurately. The $\text{Pt}(\alpha, xn)\text{Hg}^{197,197m}$ cross-section ratios are tabulated in Table IV and illustrated in Fig. 2. The three isotopes Pt^{194} , Pt^{195} , and Pt^{196} were present in approximately equal abundances in the natural platinum targets which were used. The principal reactions leading to the isomers are the $\text{Pt}^{194}(\alpha, n)$, $\text{Pt}^{195}(\alpha, 2n)$, and $\text{Pt}^{196}(\alpha, 3n)$ reactions. The threshold for the $\text{Pt}^{194}(\alpha, 3n)\text{Hg}^{195}$ reaction is approximately 25 MeV. The experiments were not extended to energies appreciably above this threshold because the Hg^{195} activities interfere with the detection of the Hg^{197} activities.

The isomeric cross-section ratios for the $\text{Hg}^{198}(n, 2n)$, $\text{Hg}^{198}(\alpha, xn)$, and $\text{Hg}^{196}(d, p)$ reactions are tabulated in Table V. When two values are listed two separate measurements have been made.

4. STATISTICAL MODEL CALCULATIONS

It can be seen from the data in Tables II–IV that as the projectile energy is increased, and thus the angular momentum in the compound nucleus is increased, the

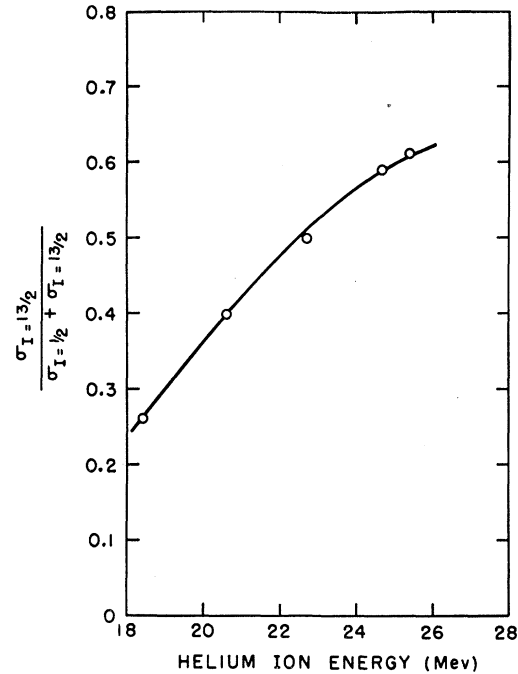


FIG. 2. Isomeric cross-section ratios, $\sigma_{I=13/2}/(\sigma_{I=1/2} + \sigma_{I=13/2})$, for the $\text{Pt}(\alpha, xn)$ reactions leading to Hg^{197} and Hg^{197m} as a function of helium ion energy.

relative yield of the high spin isomer increases. This results in an interesting displacement of the $\text{Au}^{197}(d, 2n)$ - Hg^{197m} excitation function relative to the $\text{Au}^{197}(d, 2n)$ - Hg^{197g} excitation function, as may be seen in Fig. 3. A statistical model has been used to calculate the effect of initial angular momentum on isomer yields, and to deduce information about the dependence of the nuclear level density on angular momentum.

The first step in this approach is the calculation of the distribution of the angular momentum, J_c , of the compound nucleus. This is given by^{10,11}

$$\sigma(J_c, E) = \pi \lambda^2 \sum_{S=|I-s|}^{I+s} \sum_{l=|J_c-S|}^{J_c+S} \frac{2J_c+1}{(2s+1)(2I+1)} T_l(E), \quad (2)$$

where λ is the deBroglie wavelength of the incoming

TABLE V. Isomeric cross-section ratios for various reactions producing $\text{Hg}^{197,197m}$.

Reaction	Projectile energy (MeV)	$\sigma_{I=13/2}/\sigma_{I=1/2}$
$\text{Hg}^{196}(n, \gamma)$	thermal	0.044 ± 0.008
$\text{Hg}^{196}(d, p)$	{ 11	0.15 ± 0.03
	{ 11	0.16 ± 0.03
$\text{Hg}^{198}(\alpha, \alpha n)$	{ 41	0.9 ± 0.1
	{ 41	1.0 ± 0.1
$\text{Hg}^{198}(n, 2n)$	14.1	0.8 ± 0.1

¹⁰ W. Hauser and H. Feshbach, Phys. Rev. **87**, 366 (1952).

⁹ M. L. Sehgal, H. S. Hans, and P. S. Gill, Nuclear Phys. **12**, 261 (1959).

¹¹ J. M. Blatt and V. F. Weisskopf, *Theoretical Nuclear Physics* (John Wiley & Sons, Inc., New York, 1952).

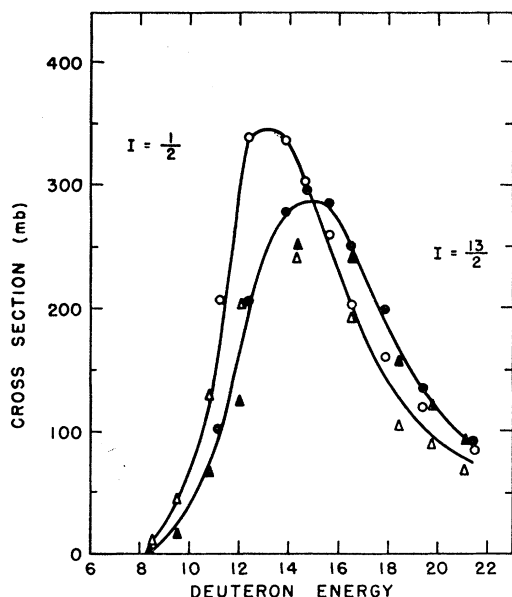


FIG. 3. Excitation functions for the $\text{Au}^{197}(d,2n)\text{Hg}^{197m}$ (solid symbols) and $\text{Au}^{197}(d,2n)\text{Hg}^{197}$ (open symbols) reactions as a function of deuteron energy. The circles and triangles refer to two separate runs.

projectile, s is the spin of the projectile, I is the spin of the target nucleus and $T_l(E)$ is the barrier transmission coefficient of a particle with orbital angular momentum l and energy E . The distributions in J_c for two deuteron energies are illustrated in Fig. 4. This expression is valid only for capture of particles, as the derivation requires the assumption that the level density of the compound nucleus does not affect the distribution of J_c values formed in the compound nucleus. It is thought that the matrix element for reaching a given state J_c of the compound nucleus from the target nucleus ground state is inversely proportional to the density of states with angular momentum $J=J_c$. One can think of the single particle strength between initial and final states being diluted according to the number of final states it is spread out over.

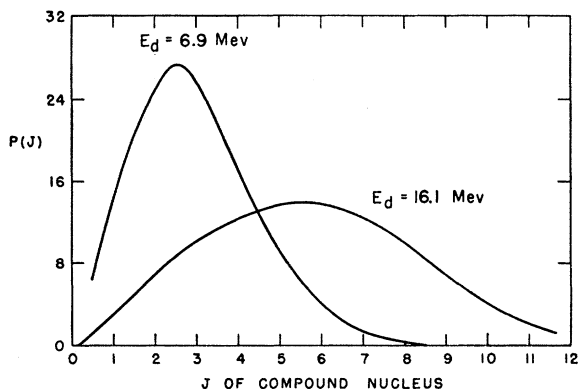


FIG. 4. The distribution in angular momenta J of the compound nucleus for two different deuteron bombarding energies.

After calculating the distribution function for the angular momentum J_c of the compound nucleus, one must examine the modification of this distribution function by emission of neutrons and finally gamma rays.

The relative probability for a compound state with angular momentum J_c to emit a neutron with orbital angular momentum l leading to a final state with angular momentum J_f is given by

$$P(J_f) \propto \rho(J_f) \sum_{S=|J_f-\frac{1}{2}|}^{J_f+\frac{1}{2}} \sum_{l=|J_c-S|}^{J_c+S} T_l(E), \quad (3)$$

where $T_l(E)$ is the barrier transmission coefficient for a neutron with orbital angular momentum l and energy E . The probability of populating a final state with spin J_f by particle emission from a compound state of spin J_c , given by Eq. (3), depends on the level density factor $\rho(J_f)$ which is given by Eq. (1). It should be mentioned, however, that Eq. (3) does not contain a factor comparable to the $2J+1$ term in the numerator of Eq. (2) which arises from considerations other than level density. For $\sigma = \infty$, which has sometimes been assumed, $\rho(J_f)$ is directly proportional to $2J_f+1$ [see Eq. (1)] and Eq. (3) resembles the form of Eq. (2) even though the $2J+1$ factors have different origins. In view of the complexity of character of both the initial and final

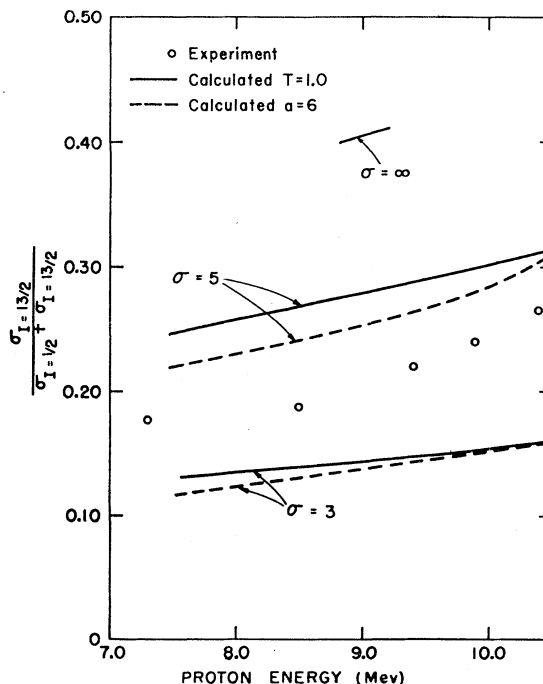


FIG. 5. Comparison of the experimental (open circles) and calculated isomeric cross-section ratios, $\sigma_{I=13/2}/(\sigma_{I=1/2} + \sigma_{I=13/2})$, for the $\text{Au}^{197}(p,n)$ reaction. The solid line curves were calculated for two values of the spin-dependence parameter σ and a constant nuclear temperature of 1 Mev for the emitted neutrons. The dashed curves were calculated assuming the nuclear temperature for the emitted neutrons varied with excitation energy as predicted by the degenerate Fermi gas model.

states, we have assumed that the matrix elements connecting the initial state of the compound nucleus and the final states following neutron emission are on the average equal.

The calculations are performed by allowing each compound state J_c to emit a neutron whose transmission coefficient T_l is taken as that for a neutron with an energy corresponding to the mean kinetic energy given by evaporation theory. This approximation was checked by breaking the neutron spectra up into four energy groups and carrying out the calculations individually for each group. It was found that using the average neutron energy was a surprisingly accurate approximation. The resulting distribution of spins is calculated for several choices of the parameter σ . If a second neutron is to be evaporated, the process is repeated. After neutron emission is energetically forbidden, the gamma-ray cascade is followed according to the procedure outlined in the preceding paper¹² and the relative populations of the two isomers are calculated. The number of gamma rays assumed to be emitted depended on the residual excitation energy following neutron emission (determined by assuming that all neutrons carried away the mean kinetic energy) and varied between one and four gamma rays per cascade.

In deciding whether the last gamma-ray transition populates the ground or metastable state, the $I=5/2$ state lying between the $I=1/2$ ground state and the $I=13/2$ metastable state must be considered. It is assumed that states with $I \geq 11/2$ populate the metastable state, states with $I \leq 7/2$ populate (directly or through the $I=5/2$ state) the ground state, and states with $I=9/2$ populate both the isomeric and ground state.

The transmission coefficients for both the incoming and outgoing particles have been calculated on the basis of a square well nuclear potential with a radius $R=1.5 \times 10^{-13} A^{1/3}$ cm. The calculations of Feshbach *et al.*¹³ have been used for the charged particles and the calculations of Feld *et al.*¹⁴ for the neutrons. Because of the unavailability of transmission coefficient calculations appropriate for the helium ion bombardments of

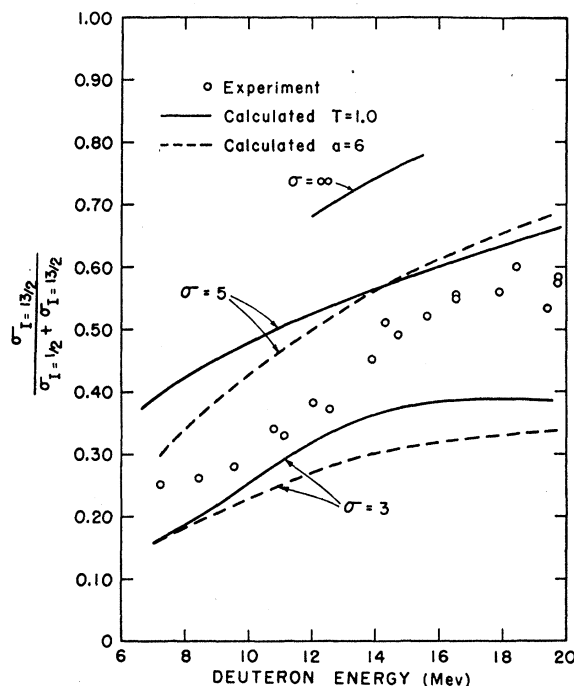


Fig. 6. Comparison of the experimental (open circles) and calculated isomeric cross-section ratios $\sigma_{I=13/2}/(\sigma_{I=1/2} + \sigma_{I=13/2})$ for the $\text{Au}^{197}(d,2n)$ reaction. The solid line curves were calculated for two values of the spin-dependence parameter σ and a constant nuclear temperature of 1 Mev for the emitted neutrons. The dashed curves were calculated assuming the nuclear temperature for the emitted neutrons varied with excitation energy as predicted by the degenerate Fermi gas model.

platinum, no calculations have been performed for this system.

The calculations have been performed for two assumptions about the energy dependence of the nuclear level density. A dependence of the form $\rho(E) \propto \exp(E/T)$ (Case A) where E is the excitation energy, gives rise to a nuclear temperature T independent of excitation energy. The dependence predicted by the Fermi gas model $\rho(E) \propto \exp[2(aE)^{1/2}]$ (Case B) corresponds to a nuclear temperature given by $T=(E/a)^{1/2}$. The choice of the energy dependence of the level density affects the calculations only in the mean kinetic energy carried off by the neutrons and to a lesser extent in the number of gamma rays in the final gamma-ray cascade (any dependence of σ on temperature has been neglected). Calculations were performed for Case A with a nuclear temperature $T=1.0$ Mev and for Case B with the parameter $a=6$. It can be seen from Figs. 5 and 6 and Table VI that the calculations are rather insensitive to the choice of the dependence of the level density on excitation energy. The calculations have also been found to be rather insensitive to the absolute value of the nuclear temperature. As was mentioned in the previous paper, a slight ambiguity may arise from the model dependence of the $f(E, B, J_c, J_f)$ factor in the expression for the radiation width [see Eq. (1), preceding paper]. The results of the

TABLE VI. Comparison of calculated and experimental isomeric cross-section ratios for the $\text{Hg}^{198}(n,2n)$ reaction.

$\text{Hg}^{198}(n,2n)$	$\sigma_{I=13/2}/(\sigma_{I=1/2} + \sigma_{I=13/2})$	
Experimental	0.44 ± 0.05	
Calculated	$\sigma=3$	$\sigma=5$
Case A	0.32	0.60
Case B	0.35	0.63

¹² J. R. Huizenga and R. Vandenbosch, preceding paper [Phys. Rev. 120, 1305 (1960)].

¹³ H. Feshbach, M. M. Shapiro, and V. F. Weisskopf, Atomic Energy Commission Report NYO-3077, 1953 (unpublished).

¹⁴ B. T. Feld, H. Feshbach, M. L. Goldberger, H. Goldstein, and V. F. Weisskopf, Atomic Energy Commission Report NYO-636 1951 (unpublished).

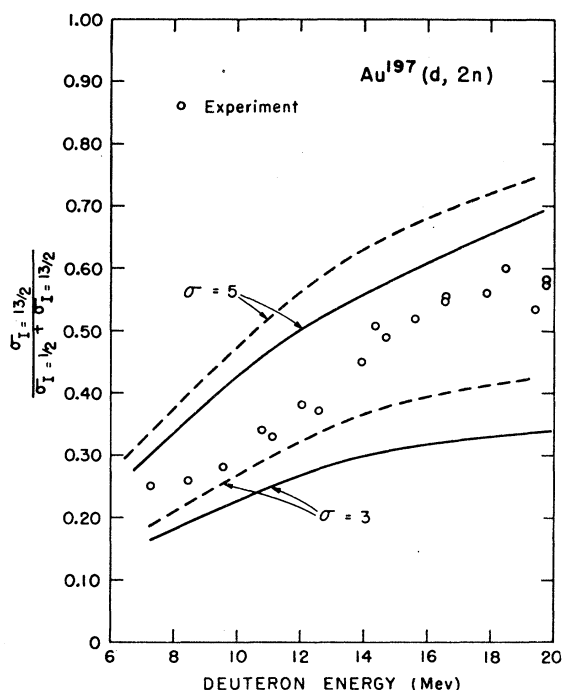


FIG. 7. Comparison of the calculated isomeric cross-section ratios for two assumptions about the J dependence of the $f(E, B, J_e, J_f)$ factor in the expression for the radiation width [see Eq. (1), preceding paper and discussion in text of this and preceding paper]. The solid line was computed assuming $f(E, B, J_e, J_f)$ is equal to unity, and the dashed line was computed assuming $f(E, B, J_e, J_f)$ is proportional to $2J_f + 1$.

calculations shown in Figs. 5 and 6 and Table VI have been obtained with the assumption that the factor $f(E, B, J_e, J_f)$ is equal to unity. The results derived with this assumption have been compared in Fig. 7 with those derived from the somewhat arbitrary assumption introduced in the preceding paper that $f(E, B, J_e, J_f)$ is proportional to $2J_f + 1$. The general result is that σ is reduced by one unit or less for the latter assumption, so that uncertainties of this nature in treating the gamma-ray cascade do not seriously affect the choice of σ .

Two important conclusions can be drawn from the comparison of these calculations with the experimental results. In the first place, it is seen that the same value of σ is obtained irrespective of whether the reaction leading to the products is a (p, n) , $(d, 2n)$, or $(n, 2n)$. This provides evidence in support of the compound nucleus model, if one characterizes the compound nucleus by its angular momentum J_e as well as its excitation energy. Secondly, it is seen that analysis of isomeric cross-section ratios can provide information about the spin dependence of the nuclear level density. The value of σ deduced here, $\sigma = 4 \pm 1$ for mass number $A \simeq 200$, is similar to the values of σ which have been deduced^{4,5} for $A \leq 60$. Other than those derived in the accompanying paper, there

have not been any determinations of σ for $A > 60$ reported. Since $\sigma^2 = Tg/\hbar^2$, we obtain an effective moment of inertia for $A \simeq 200$ from the determination of σ . With $\sigma = 4$ and $T = 1$ Mev, the ratio of the effective moment of inertia to the rigid body moment of inertia is about 0.1.

It has been assumed throughout the calculations that σ is independent of excitation energy. As can be seen from Figs. 5 and 6, the σ determined for different bombarding energies is rather constant, indicating that the assumption is a good first approximation. Since at a fixed bombarding energy the de-excitation processes sample the level density at several different excitation energies, a more detailed analysis than given here is required to obtain quantitative information on the variation of σ with excitation energy. There is some indication from Fig. 6 that σ may increase slightly with excitation energy, but it would seem to be a weak dependence.

5. DIRECT INTERACTIONS

The low value, $\sigma_m/\sigma_g = 0.15$, of the isomeric cross-section ratio for the $Hg^{198}(d, p)$ reaction is not surprising, as this reaction is known to proceed primarily by a stripping mechanism. This mechanism does not require that the full angular momentum brought in by the deuteron be transferred to the residual nucleus, as the proton carries away much of the incident energy.

The isomeric cross-section ratio for the $Hg^{198}(\alpha, \alpha n)$ reaction is rather interesting and enables one to say something about the mechanism of this reaction. The observed ratio, $\sigma_m/\sigma_g = 0.95$, is much too large to be accounted for by dipole or quadrupole Coulomb excitation followed by evaporation of a neutron. The isomeric cross-section ratio to be expected for inelastic scattering where both the alpha particle and the neutron are evaporated from a compound nucleus is somewhat more difficult to predict, but might be expected to be rather large. A direct interaction mechanism in which a neutron is knocked out from the surface of the nucleus does not seem likely in view of the low ratio of the $(\alpha, \alpha p)$ to $(\alpha, \alpha n)$ cross sections in this mass region.^{15,16} Perhaps a more likely mechanism is a direct interaction mechanism in which the alpha particle transfers a portion of its kinetic energy and angular momentum to the nucleus which then evaporates a neutron.

ACKNOWLEDGMENTS

The authors are indebted to W. J. Ramler and the members of his cyclotron group for performing the cyclotron irradiations, and to Harvey Casson for the 14.1-Mev neutron irradiation. Helpful discussions with P. Axel and H. Warhanek are gratefully acknowledged.

¹⁵ R. Vandenbosch (unpublished).

¹⁶ B. M. Foreman, Jr., Bull. Am. Phys. Soc. 5, 270 (1960).